The *closo*-$[Sn_9M(CO)_3]^{4-}$ Zintl Ion Clusters where M = Cr, Mo, W: Two Structural Isomers and Their Dynamic Behavior

Banu Kesanli, James Fettinger, and Bryan Eichhorn*[a]

Abstract: The *closo*-$[Sn_9M(CO)_3]^{4-}$ ions where M = Cr (**1**), Mo (**2**), W (**3**) were prepared from $[LM(CO)_3]$ precursors (L = mesitylene, cycloheptatriene), K_4Sn_9, and 2,2,2-cryptand in ethylenediamine/toluene solvent mixtures. The $[K(2,2,2\text{-cryptand})]^+$ salts are very air and moisture sensitive and have been characterized by IR, ^{119}Sn, and ^{13}C NMR spectroscopy and single-crystal X-ray diffraction studies. Complexes **1**–**3** form bicapped square-antiprismatic 10-vertex 22-electron *closo* structures in which the $\{M(CO)_3\}$ units occupy cluster vertices. For **1** and **2**, the clusters have C_{4v} symmetry in the solid state in which the $\{M(CO)_3\}$ fragments occupy capping positions with Sn_9^{4-} ions that are bound to the metal in an η^4 fashion. For **3**, the $\{M(CO)_3\}$ fragment occupies a position in the square plane with an η^5-Sn_9^{4-} ion and C_s point symmetry. For **1**–**3**, a dynamic equilibrium exists between the η^4 and η^5 structures yielding three ^{119}Sn NMR signals that reflect the three chemically distinct Sn environments of the higher symmetry C_{4v} structure. The ^{119}Sn NMR chemical shifts and coupling constants show solvent and temperature dependencies due to the equilibrium process. A triangular-face rotation mechanism is proposed to describe the dynamic behavior.

Keywords: coordination complexes · dynamic properties · NMR spectroscopy · structure elucidation · Zintl anions

Introduction

The synthesis of the first nine-atom Zintl ion, Pb_9^{4-}, was first accomplished by Joannis in 1891,[1, 2] but the charge and actual identity of this cluster and the tin analogue, Sn_9^{4-}, was determined by Kraus, Smyth,[3–5] and Zintl himself[6–9] in the early 1900's. The single-crystal X-ray study of the $[Na_4Sn_9(en)_7]$ by Kummer et al.[10] confirmed the Zintl–Kraus cluster models and provided the first structural data for this class of deltahedral cluster anions.[11, 12] Sn_9^{4-} adopts a discrete 9-vertex, 22-electron structure with C_{4v} point symmetry (see **I**) and is classified as a *nido* cluster type according to Wade's Rules.[13] Following these structural investigations, Rudolph and co-workers studied the solution dynamics of *nido*-Sn_9^{4-} by way of ^{119}Sn NMR spectroscopy.[14] Their studies showed that, unlike the isoelectronic boranes, *nido*-Sn_9^{4-} is highly fluxional in solution such that all nine Sn atoms are in rapid exchange on the NMR timescale at −74 °C. The presence and intensity of ^{117}Sn satellites on the lone resonance indicates that the exchange is intramolecular.[12, 15] The mechanism of exchange was described by Corbett[11, 12] and involves a bond-making step across the open face of the cluster along with a bond-breaking process at the opposite end of the cluster (see Scheme 1). Subsequent to the studies on *nido*-Sn_9^{4-}, other related Zintl ions were isolated and structurally characterized.[16] They include *nido*/*closo*-Sn_9^{3-} (see **II**),[17, 18] *closo*-Sn_5^{2-},[19] Sn_4^{2-},[20] and various solid state species[21] including the $K_{12}Sn_{17}$ phase with isolated *nido*-Sn_9^{4-} clusters.[22]

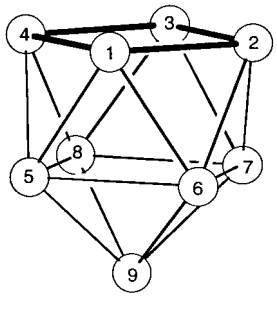

I

Metallated polystannides have been prepared by various means and include the complexes *closo*-$[Sn_9Cr(CO)_3]^{4-}$[23] and *closo*-$[Sn_6\{Cr(CO)_5\}_6]^{2-}$.[24, 25] The Cr atom in the former caps the open square face of *nido*-Sn_9^{4-} (see bold lines in **I**) to form a 10-atom 22-electron *closo*-cluster, whereas the $\{Cr(CO)_5\}$ fragments of the latter are exopolyhedral groups on the octahedral *closo*-Sn_6^{2-} core. More recently, we have shown that *nido*-Sn_9^{4-} reacts with $[Nb(\eta\text{-}C_7H_8)_2]$ to give $[(\eta\text{-}C_7H_8)Nb(cyclo\text{-}Sn_6)Nb(\eta\text{-}C_7H_8)]^{2-}$ that contains two-center two-electron bonds.[26] This complex and *closo*-$[Sn_6\{Cr(CO)_5\}_6]^{2-}$ are static on the NMR timescale,[25] as expected, and show one-bond Sn–Sn coupling constants significantly larger that those of *nido*-Sn_9^{4-}.[12, 15]

[a] Prof. B. Eichhorn, B. Kesanli, Dr. J. Fettinger
Department of Chemistry and Biochemistry
University of Maryland, College Park, Maryland 20742 (USA)
Fax: (+1) 301-314-9121
E-mail: b.eichhorn@umail.umd.edu

Supporting information for this article is available on the WWW under http://www.wiley-vch.de/home/chemistry/ or from the author.

  0947-6539/01/0724-5277 $ 17.50+.50/0

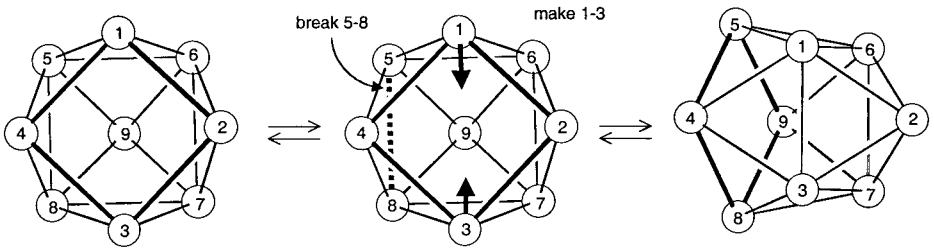

Scheme 1.

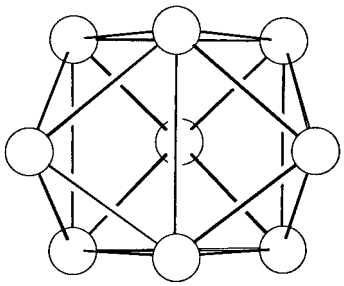

II

The first metallated Zintl ion, a Sn_9^{4-}–$Pt(PPh_3)_x$ complex characterized by ^{119}Sn NMR spectroscopy, was detected by Rudolph and co-workers in a reaction between *nido*-Sn_9^{4-} and $[Pt(PPh_3)_4]$.[27] The presence of ^{195}Pt–^{119}Sn coupling observed in the room temperature ^{119}Sn NMR spectrum indicates that the $\{Pt(PPh_3)_x\}$ fragment does not dissociate from the Sn_9 cluster on the NMR timescale. However, the complex is highly fluxional and shows a single time-averaged chemical shift for the nine tin atoms.[27] Because the composition and structure of the complex remain unknown, one cannot speculate about the mechanism of the dynamic behavior. It was surprising to us that the proposed[27] *nido*-10-atom 24-electron cluster would retain dynamic behavior similar to *nido*-Sn_9^{4-} with global exchange of all nine Sn atoms. The familiar square–diamond–square exchange mechanism available to the *nido* structures (i.e. Scheme 1)[16] is not expected for the metallated species and different fluxional processes may be operative. This observation prompted us to study the relationships between the structures of the metallated Sn_9 complexes and their dynamic behavior. In a subsequent publication, we will describe the dynamic behavior of the Rudolph complex and its subsequent Pt insertion product, $[Sn_9Pt_2(PPh_3)]^{2-}$.[28] Herein we describe the synthesis, structures, properties, and solution dynamics of the *closo*-$[Sn_9M(CO)_3]^{4-}$ ions in which M = Cr, Mo, W. The structure of one polymorph of *closo*-$[Sn_9Cr(CO)_3]^{4-}$ was previously communicated.[23] In this study, we describe a new isomeric form of the *closo*-$[Sn_9M(CO)_3]^{4-}$ structure in both the solid state and in solution. The dynamic behavior of the *closo*-$[Sn_9M(CO)_3]^{4-}$ ions differs significantly from the Pt–Sn_9 complexes and the *nido*-Sn_9^{4-} ion. Immediately prior to the submission of this manuscript, we learned that Schrobilgen et al. had also characterized the Mo and W *closo*-$[Sn_9M(CO)_3]^{4-}$ ions, which will be described in a subsequent publication.[29]

Results

Synthesis: Solutions of K_4Sn_9 in ethylenediamine (en) react with solutions of $LM(CO)_3$ (where M = Cr, Mo, W; L = mesitylene, cycloheptatriene) in toluene (tol) in the presence of 2,2,2-cryptand to give moderate yields of the *closo*-$[Sn_9M(CO)_3]^{4-}$ complexes as the $[K(2,2,2\text{-crypt})]^+$ salts [Eq. (1)].

$$K_4Sn_9 + [M(CO)_3L] + 4\,(2,2,2\text{-crypt}) \longrightarrow [K(2,2,2\text{-crypt})]_4[Sn_9M(CO)_3] + L \quad (1)$$

In Equation (1) M = Cr and L = $C_6H_3Me_3$ for complex **1**, M = Mo and L = cycloheptatriene for complex **2**, and M = W, L = $C_6H_3Me_3$ for compound **3**. The crystalline solids of the *closo*-$[Sn_9Cr(CO)_3]^{4-}$ ion (**1**) form very dark red-brown needles, whereas the *closo*-$[Sn_9Mo(CO)_3]^{4-}$ (**2**) and *closo*-$[Sn_9W(CO)_3]^{4-}$ (**3**) ions form dark red-brown blocks. The three complexes are very air and moisture sensitive in solution and the solid state. The salts are sparingly soluble in en, moderately soluble in DMF and CH_3CN, and form dark red-brown solutions. The complexes have been characterized by single-crystal X-ray diffraction, IR, ^{13}C, and ^{119}Sn NMR spectroscopy, and elemental analysis.

Two different isomeric forms of the $[Sn_9M(CO)_3]^{4-}$ ions are observed in the solid state, the "η^4 structure" and the "η^5 structure" that rapidly interconvert in solution. Details of the structures and the dynamic equilibria are described in the next two sections.

Crystalline samples of $[K(2,2,2\text{-crypt})]_4[Sn_9W(CO)_3]$ isolated from en/tol solvent mixtures are composed of dark chunky crystals of different sizes along with somewhat lighter glassy blocks that did not diffract. IR analysis (KBr pellets) of bulk crystalline products from several reactions showed mixtures of the η^5 complex (ν_{CO} = 1805, 1701 cm^{-1}) and the η^4 complex (ν_{CO} = 1822, 1705 cm^{-1}) in ratios that vary from 1:2 to 2:1. Single-crystal analysis of several dark chunky crystals of different sizes showed them all to be the η^5 complex. The η^4 complex crystallizes preferentially (but not exclusively) from the THF/en solvent mixtures.[29] To date, all samples of crystalline $[K(2,2,2\text{-crypt})]_4[Sn_9W(CO)_3]$ isolated in our laboratories have been mixtures of the η^4 and η^5 isomers (solid-state IR analysis).

Solid-state structures: The $[K(2,2,2\text{-crypt})]_4[Sn_9Cr(CO)_3]$ salt crystallizes in three different polymorphs that differ only by the solvate molecules in the crystal lattice. All three polymorphs crystallize under identical synthetic conditions. The previously reported polymorph[23] contains a doubled unit cell with eight $[K(2,2,2\text{-crypt})]^+$ and two $[Sn_9Cr(CO)_3]^{4-}$ independent ions with monoclinic $P2_1/c$ crystal symmetry. In addition, there are unresolved solvate molecules in the crystal lattice that are not within bonding distance of the anions.[23] The two new polymorphs reported here are triclinic, space group $P\bar{1}$. One polymorph contains 1.5 en solvates per cluster, whereas the other is solvate-free. Summaries of the crystal data for the triclinic structures are given in Table 1. All of the

0947-6539/01/0724-5278 $ 17.50+.50/0 *Chem. Eur. J.* **2001**, *7*, No. 24

Table 1. Crystallographic data for the $[K(2,2,2\text{-crypt})]_4[Sn_9M(CO)_3]$ salts in which M = Cr, W.

	$[K(2,2,2\text{-crypt})]_4$[**1**] · 1.5 en	$[K(2,2,2\text{-crypt})]_4$[**1**]	$[K(2,2,2\text{-crypt})]_4$[**3**] · 1.5 en
formula	$C_{78}H_{156}CrK_4N_{11}O_{27}Sn_9$	$C_{75}H_{144}CrK_4N_8O_{27}Sn_9$	$C_{78}H_{156}WK_4N_{11}O_{27}Sn_9$
M_r	2956.75	2866.59	3088.60
T [K]	193(2)	193(2)	193(2)
λ [Å]	0.71073	0.71073	0.71073
crystal system	triclinic	triclinic	triclinic
space group	$P\bar{1}$	$P\bar{1}$	$P\bar{1}$
a [Å]	15.6668(5)	15.0097(5)	15.5011(13)
b [Å]	16.0478(5)	16.8423(6)	16.6537(14)
c [Å]	25.9299(9)	24.0980(8)	25.651(2)
α [°]	94.1750(10)	90.7360(10)	79.4730(10)
β [°]	90.6020(10)	99.1950(10)	75.2150(10)
γ [°]	118.5810(10)	114.6260(10)	63.0930(10)
V [Å^3]	5702.0(3)	5445.2(3)	5692.0(8)
Z	2	2	2
ρ_{calcd} [g cm^{-3}]	1.722	1.748	1.802
μ [mm^{-1}]	2.240	2.342	3.158
crystal size [mm]	0.296 × 0.243 × 0.175	0.35 × 0.20 × 0.03	0.183 × 0.091 × 0.055
θ range [°]	1.58–27.50	0.86–25.00	1.50–25.00
index ranges	$-20 \le h \le 20$	$-17 \le h \le 17$	$-18 \le h \le 18$
	$-20 \le k \le 20$	$-20 \le k \le 19$	$-19 \le k \le 19$
	$-33 \le l \le 33$	$-28 \le l \le 28$	$-30 \le l \le 30$
reflections collected	90485	58522	74103
independent reflections	26037 [R(int) = 0.0347]	19170 [R(int) = 0.0856]	20049 [R(int) = 0.0887]
goodness-of-fit on F^2	1.030	0.963	1.076
final R [$I > 2\sigma(I)$][a]	$R1 = 0.0364$, $wR2 = 0.0846$	$R1 = 0.0445$, $wR2 = 0.0608$	$R1 = 0.0592$, $wR2 = 0.1272$
R indices (all data)[a]	$R1 = 0.0562$, $wR2 = 0.0951$	$R1 = 0.1092$, $wR2 = 0.0692$	$R1 = 0.1309$, $wR2 = 0.1695$
largest peak/hole [e × Å^{-3}]	1.699/−0.716	0.810/−0.653	1.570/−1.297

[a] The function minimized during the full-matrix least-squares refinement was $\Sigma w(F_o^2 - F_c^2)$ in which $w = 1/[\sigma^2(F_o^2) + (0.0180P)^2 + 10.4114P]$ and $P = (\max(F_o^2,0) + 2 \times F_c^2)/3$.

closo-$[Sn_9Cr(CO)_3]^{4-}$ ions are identical, within experimental error, and the three structures differ only by virtue of the lattice solvates and the crystal packing. Selected bond lengths and angles for the triclinic en-solvate polymorph are given in Table 2. Structural details for the triclinic solvate-free polymorph can be obtained from the Cambridge Crystallographic Database (see crystallographic experiment). The data for the monoclinic polymorph were previously published.[23]

Table 2. Selected bond lengths [Å] and angles [°] for $[Sn_9Cr(CO)_3]^{4-}$.

Sn(1)–Cr(1)	2.8172(7)	Sn(4)–Sn(8)	2.9887(4)
Sn(2)–Cr(1)	2.8733(7)	Sn(5)–Sn(9)	2.9441(4)
Sn(3)–Cr(1)	2.8906(7)	Sn(5)–Sn(8)	3.1684(4)
Sn(4)–Cr(1)	2.8733(7)	Sn(5)–Sn(6)	3.2038(4)
Sn(1)–Sn(5)	2.9628(4)	Sn(6)–Sn(9)	2.9344(4)
Sn(1)–Sn(6)	2.9680(4)	Sn(6)–Sn(7)	3.1643(4)
Sn(1)–Sn(2)	3.0699(4)	Sn(7)–Sn(9)	2.9643(4)
Sn(1)–Sn(4)	3.0720(4)	Sn(7)–Sn(8)	3.1622(4)
Sn(2)–Sn(7)	2.9916(4)	Sn(8)–Sn(9)	2.9805(5)
Sn(2)–Sn(6)	3.0086(4)	Cr(1)–C(2)	1.791(4)
Sn(2)–-Sn(3)	3.0317(4)	Cr(1)–C(1)	1.803(4)
Sn(3)–Sn(7)	3.0070(4)	Cr(1)–C(3)	1.809(4)
Sn(3)–Sn(8)	3.0127(5)	C(1)–O(1)	1.180(5)
Sn(3)–Sn(4)	3.0348(4)	C(2)–O(2)	1.181(5)
Sn(4)–Sn(5)	2.9735(4)	C(3)–O(3)	1.181(5)
C(2)-Cr(1)-C(1)	82.26(19)	C(3)-Cr(1)-Sn(2)	128.93(15)
C(2)-Cr(1)-C(3)	90.90(19)	O(1)-C(1)-Cr(1)	173.2(4)
C(1)-Cr(1)-C(3)	89.6(2)	O(2)-C(2)-Cr(1)	173.1(3)
C(2)-Cr(1)-Sn(1)	104.26(13)	O(3)-C(3)-Cr(1)	175.3(4)
C(1)-Cr(1)-Sn(1)	82.51(13)	Sn(2)-Sn(1)-Sn(4)	90.038(10)
C(3)-Cr(1)-Sn(1)	161.73(14)	Sn(3)-Sn(2)-Sn(1)	89.292(10)
C(2)-Cr(1)-Sn(4)	169.23(13)	Sn(2)-Sn(3)-Sn(4)	91.473(10)
C(1)-Cr(1)-Sn(4)	93.19(14)	Sn(3)-Sn(4)-Sn(1)	89.196(10)
C(3)-Cr(1)-Sn(4)	98.86(14)	Sn(8)-Sn(5)-Sn(6)	89.901(10)
Sn(1)-Cr(1)-Sn(4)	65.338(15)	Sn(7)-Sn(6)-Sn(5)	89.345(10)
C(2)-Cr(1)-Sn(2)	78.88(12)	Sn(8)-Sn(7)-Sn(6)	90.732(10)
C(1)-Cr(1)-Sn(2)	136.75(15)	Sn(7)-Sn(8)-Sn(5)	90.020(10)

The structure of the anion **1** (Figure 1) is composed of a symmetrical 10-vertex 22-electron *closo* deltahedron in accordance with Wade's rules of electron counting.[13] The Cr and the Sn(9) atoms occupy capping positions of the bicapped square antiprism and are bound to only four other vertices. The other eight Sn atoms are in the square planes (the waist positions) and are five coordinate. When viewed as a metal–ligand complex, the Sn_9^{4-} ion is bound in an η^4 fashion to the $\{Cr(CO)_3\}$ fragment. This isomer is designated as the "η^4 structure".[30] The Cr–Sn bonds average 2.86(5) Å with three contacts between 2.8733(7)–2.8906(7) Å and a shorter bond to Sn1 of 2.8172(7) Å. The latter occurs despite the virtually *trans* orientation of the C(3) carbonyl carbon atom [Sn1–Cr–C3 = 161.7(1)°] which results in bond lengthening in the related polypnictide complexes.[31] The Sn–Sn bonds are in the range 2.9628(4)–3.0720(4) Å except for those within the bottom square plane (Sn5–Sn6–Sn7–Sn8), which are slightly longer (3.1622(4)–3.2038(4) Å). The regular nature of the square antiprism (Figure 1, right) is evidenced by the narrow range of Sn–Sn–Sn bond angles within the square planes (90.0 ± 1.5°). The differences in the Sn–Sn contacts within the upper and lower square planes are also observed and are more pronounced in *nido*-Sn_9^{4-}.[11]

Crystals of the $[K(2,2,2\text{-crypt})]_4[Sn_9Mo(CO)_3] \cdot 1.5\,en$ are isomorphic with the Cr analogue described above and contain an $[\eta^4\text{-}Sn_9Mo(CO)_3]^{4-}$ cluster.[32] Schrobilgen et al. have characterized a different polymorph of the same cluster and will describe the details of its structure in a subsequent publication.[29]

The $[K(2,2,2\text{-crypt})]_4[Sn_9W(CO)_3] \cdot 1.5\,en$ salt is triclinic, space group $P\bar{1}$, and contains a disordered en solvate molecule in the crystal lattice. A summary of the crystal data is given in Table 1 and selected bond lengths and angles are given in Table 3.

The $[Sn_9W(CO)_3]^{4-}$ anion (**3**) (Figure 2) also adopts a symmetrical 10-vertex 22-electron *closo* deltahedral structure in accordance with Wade's rules. However, the $\{W(CO)_3\}$ unit occupies a vertex in the waist position rather than a capping position as found in **1**. In the waist position, the tungsten atom attains a higher coordination number due to the η^5 coordination of the Sn_9 cluster. This new isomer is designated as the "η^5

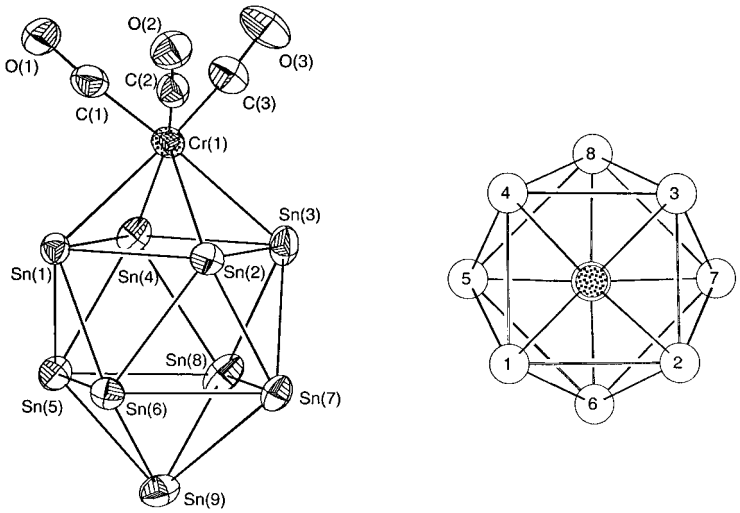

Figure 1. Left: ORTEP drawing of the $[Sn_9Cr(CO)_3]^{4-}$ ion (**1**). Right: A top view with the carbonyl groups omitted.

Table 3. Selected bond lengths [Å] and angles [°] for the *closo*-$[Sn_9W(CO)_3]^{4-}$ ion.

W(1)−C(3)	1.907(15)	Sn(2)−Sn(7)	3.0495(15)
W(1)−C(2)	1.952(18)	Sn(2)−Sn(3)	3.1935(16)
W(1)−C(1)	1.975(18)	Sn(3)−Sn(7)	2.9314(15)
W(1)−Sn(1)	2.9077(12)	Sn(3)−Sn(8)	2.9679(18)
W(1)−Sn(6)	2.9721(11)	Sn(3)−Sn(4)	3.1927(17)
W(1)−Sn(5)	2.9848(12)	Sn(4)−Sn(5)	2.9217(18)
W(1)−Sn(2)	3.1111(11)	Sn(4)−Sn(8)	3.0257(16)
W(1)−Sn(4)	3.1336(12)	Sn(5)−Sn(9)	2.9735(15)
C(1)−O(1)	1.147(18)	Sn(5)−Sn(6)	3.1377(15)
C(2)−O(2)	1.183(18)	Sn(5)−Sn(8)	3.2935(16)
C(3)−O(3)	1.237(16)	Sn(6)−Sn(9)	2.9617(15)
Sn(1)−Sn(2)	2.9330(16)	Sn(6)−Sn(7)	3.2718(14)
Sn(1)−Sn(4)	2.943(2)	Sn(7)−Sn(9)	2.9497(15)
Sn(1)−Sn(3)	3.0729(16)	Sn(7)−Sn(8)	3.1178(15)
Sn(2)−Sn(6)	2.8968(14)	Sn(8)−Sn(9)	2.9357(17)
C(3)-W(1)-C(2)	89.6(7)	Sn(1)-W(1)-Sn(4)	58.17(4)
C(3)-W(1)-C(1)	92.1(6)	Sn(6)-W(1)-Sn(4)	100.44(3)
C(2)-W(1)-C(1)	88.1(7)	Sn(5)-W(1)-Sn(4)	56.99(4)
C(3)-W(1)-Sn(1)	170.3(4)	Sn(2)-W(1)-Sn(4)	88.68(3)
C(2)-W(1)-Sn(1)	83.4(5)	O(1)-C(1)-W(1)	175.4(14)
C(3)-W(1)-Sn(6)	76.8(3)	O(2)-C(2)-W(1)	176.0(14)
C(2)-W(1)-Sn(6)	102.3(5)	O(3)-C(3)-W(1)	175.0(14)
C(1)-W(1)-Sn(6)	164.6(5)	Sn(2)-W(1)-Sn(4)	88.68(3)
Sn(1)-W(1)-Sn(6)	111.22(3)	W(1)-Sn(2)-Sn(3)	92.74(4)
C(3)-W(1)-Sn(5)	76.5(4)	Sn(4)-Sn(3)-Sn(2)	86.23(4)
C(2)-W(1)-Sn(5)	161.8(5)	W(1)-Sn(4)-Sn(3)	92.33(4)
C(1)-W(1)-Sn(5)	103.7(5)	Sn(6)-Sn(5)-Sn(8)	89.24(4)
Sn(1)-W(1)-Sn(5)	111.72(4)	Sn(5)-Sn(6)-Sn(7)	90.41(4)
Sn(6)-W(1)-Sn(5)	63.57(3)	Sn(8)-Sn(7)-Sn(6)	89.98(4)
C(3)-W(1)-Sn(2)	126.7(4)	Sn(7)-Sn(8)-Sn(5)	90.36(4)
C(2)-W(1)-Sn(2)	77.5(5)		

structure".[33] Complex **3** has no crystallographic symmetry in the solid state and only approximate C_s symmetry. The similarities in atomic radii of Sn and W give rise to similar bond length ranges; W−Sn = 2.907(1) – 3.133(2), Sn−Sn = 2.932(1) – 3.118(1) Å. A view down the capping axis (Figure 2, right) shows that the square-antiprismatic arrangement remains quite regular despite the insertion of the $\{W(CO)_3\}$ moiety. The angles within the top square plane ($90.0 \pm 6.5°$) display a larger range than those in the bottom square plane ($90.0 \pm 1.2°$), but the cluster is otherwise quite regular in shape. The bond lengths within the square planes are again approximately 0.1 Å longer on average than those between the planes or to the capping Sn atoms.

Due to the high quality of the X-ray diffraction studies, the M−C and C−O bond lengths were of significant precision so that comparisons with other related systems can be made. For the neutral $[(\eta\text{-}C_6H_6)\text{-}Cr(CO)_3]$ complex, the carbonyl Cr−C and C−O bond lengths average 1.841 Å and 1.158 Å. In the $[E_7Cr(CO)_3]^{3-}$ ions (E = P, As, Sb),[31] these distances are shortened and lengthened, respectively, due to extensive charge transfer from the Zintl ion to the $\{Cr(CO)_3\}$ fragments and subsequent π back-bonding. The Cr−C and C−O distances in **1** (1.80(1) and 1.181(2) Å, average, respectively) are indicative of a highly charged $\{Cr(CO)_3\}$ fragment that is similar to those in the $[E_7Cr(CO)_3]^{3-}$ ions.[31] The W−C and C−O bond lengths for **3** (1.95(3) and 1.19(5) Å, average, respectively) show a similar trend. This conclusion is consistent with expectation based on the charges of the complexes and electronegativities of the respective Zintl anions and is supported by spectroscopic measurements (see next section).

Solution studies: The η^4 and η^5 complexes are in equilibrium in solution and their co-crystallization does not represent an incomplete, irreversible thermal conversion of a kinetic product (i.e., the η^4 isomer) to a thermodynamic product (i.e., the η^5 isomer). This conclusion is based on the following results and observations:

1) Crystalline samples containing approximately 1:2 mixtures of the η^4 and η^5 isomers of **3** (solid-state IR analysis, see Figure 5 later) dissolve to give *one* set of ^{119}Sn NMR resonances and, more importantly, a *single* carbonyl ^{13}C NMR resonance ($\delta = 239$, $^1J(^{13}C,^{183}W) = 186$ Hz). The ^{119}Sn and ^{13}C NMR spectra of the pure, crystalline η^4 sample are identical to those of the mixed isomer samples.
2) After 16 h, an approximate 14% yield of crystalline η^5-**3** is isolated from solution (estimated from IR). If this yield represents a first-order conversion of the kinetic η^4 isomer to the thermodynamic η^5 isomer, the half-life for the conversion is approximately 74 h. However, reactions run for 336 h (> four ½ lives) show almost exclusively the η^4 isomer (> 90%) upon evaporation of the solvent (solid-state IR analysis). This result indicates that the η^4 and η^5 isomers are in equilibrium and do not represent kinetic and thermodynamic products of an irreversible transformation. The relative ratios of isomers that crystallize from solution are variable and depend on the relative rates of nucleation.

0947-6539/01/0724-5280 $ 17.50+.50/0 *Chem. Eur. J.* **2001**, *7*, No. 24

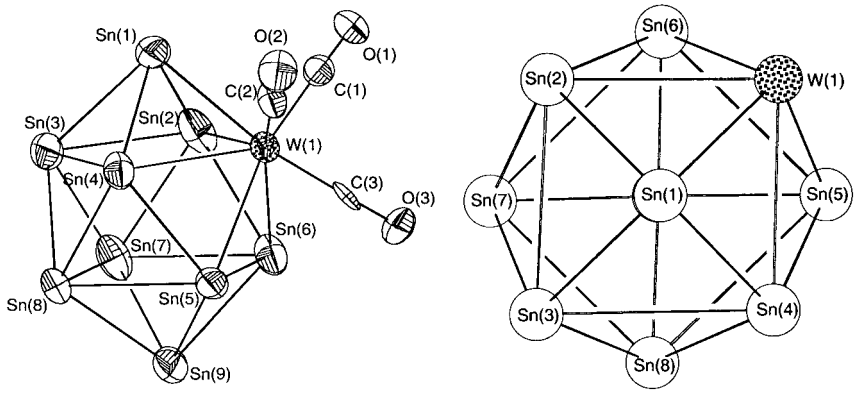

Figure 2. Left: ORTEP drawing of the $[Sn_9W(CO)_3]^{4-}$ ion (**3**). Right: A top view with the carbonyl groups omitted.

3) The chemical shifts and, more importantly, the Sn–Sn coupling constants show temperature and solvent dependencies consistent with equilibrium mixtures of isomers.[29]

The spectroscopic data supporting these conclusions are given below.

NMR spectroscopy: A summary of the ^{119}Sn NMR data for complexes **1**–**3** is given in Table 4 in the Supporting Information. The ^{119}Sn NMR spectrum of *closo*-$[Sn_9Cr(CO)_3]^{4-}$ (**1**) shown in Figure 3, displays three resonances in a 1:4:4 integral ratio at $\delta = +2327$, -180, and -447, respectively. The spectrum is consistent with expectations based on the solid-state structure and does not change significantly from room temperature to $-50\,^{\circ}$C. However, the spectrum most likely results from a dynamic equilibrium mixture of the η^4 and η^5 structures of **1** in which the equilibrium constant favors the capping η^4 structure observed in the solid state. The reasons leading us to this conclusion are described at the end of this section.

Each of the three resonances for **1** shows complicated satellite structures arising from the various isotopomers that contain statistical mixtures of naturally-abundant ^{119}Sn and ^{117}Sn nuclei (^{119}Sn, $I = 1/2$, 8.7% abundance; ^{117}Sn, $I = 1/2$, 7.7% abundance). These satellite structures are composed of first- and second-order components that complicate the quantitative evaluation of Sn–Sn coupling constants. However, the peak assignments are straightforward and can be made as follows. Based on the relative peak intensities, the downfield resonance of intensity one can be assigned to the capping Sn atom (see Sn(9) in Figure 1). This resonance shows a large splitting of 1240 Hz ($\sim {}^1J(^{119}\mathrm{Sn},^{119/117}\mathrm{Sn})$, DMF, 25 °C) which is also observed on the $\delta = -447$ resonance. Therefore, the $\delta = -447$ resonance can be assigned to the Sn atoms of the "lower waist" defined by Sn(5), Sn(6), Sn(7), and Sn(8). The remaining peak at $\delta = -180$ is, therefore, assigned to the Cr-capped square plane atoms Sn(1), Sn(2), Sn(3), and Sn(4). There is a somewhat smaller splitting of 878 Hz that the two upfield peaks share in common which we assign to ${}^1J(^{119}\mathrm{Sn},^{119/117}\mathrm{Sn})$. The smaller coupling constant is consistent with the higher coordination numbers of these tin atoms relative to the four-coordinate Sn(9) atom and the equilibrium between the η^4 and η^5 isomers. A detailed evaluation of the first- and second-order components of this complex will be reported by Schrobilgen et al. in a subsequent publication.[29]

The ^{119}Sn NMR spectrum of $[Sn_9W(CO)_3]^{4-}$ (**3**), shown in Figure 4, also has three resonances, at $\delta = +2279$, -443 and -662 with relative intensities 1:4:4, respectively (DMF, 25 °C). However, the general appearance of these resonances and their coupling constants differ from those of **1**. The solid-state structure of **3** has virtual C_s symmetry, with three unique Sn atoms that reside in the virtual mirror plane (Sn(1), Sn(3), and Sn(9)) and three pairs of chemically equivalent Sn atoms (see Figure 2, right). At least six resonances are expected on the basis of the solid-state structure, but only three resonances are observed down to $-50\,^{\circ}$C (DMF/tol mixture, 186.5 MHz) indicating that a facile dynamic exchange process is operative. Two of the peaks, those of the bottom capping Sn resonance (Sn(9), $\delta = +2279$) and the resonance for the four Sn atoms in the bottom waist (Sn(5), Sn(6), Sn(7), and Sn(8), $\delta = -662$), respectively, can be assigned according to the criteria described above for **1**. The third peak at $\delta = -443$ results from a dynamic exchange between the three Sn atoms in the top waist (Sn(2), Sn(3), Sn(4)) and the top capping atom (Sn(1)).

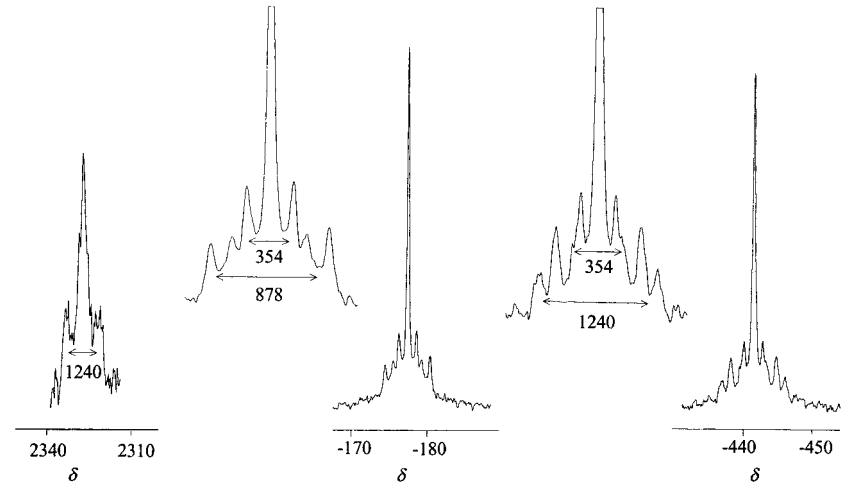

Figure 3. ^{119}Sn NMR spectra for the $[Sn_9Cr(CO)_3]^{4-}$ ion (**1**). Data were recorded at 298 K at 149.2 MHz in DMF.

The $[Sn_9Mo(CO)_3]^{4-}$ ion (**2**), is also fluxional on the NMR timescale, and three ^{119}Sn NMR resonances with satellite patterns and coupling constants that are virtually identical to that of **3** are observed. The similarity of the satellite pat-

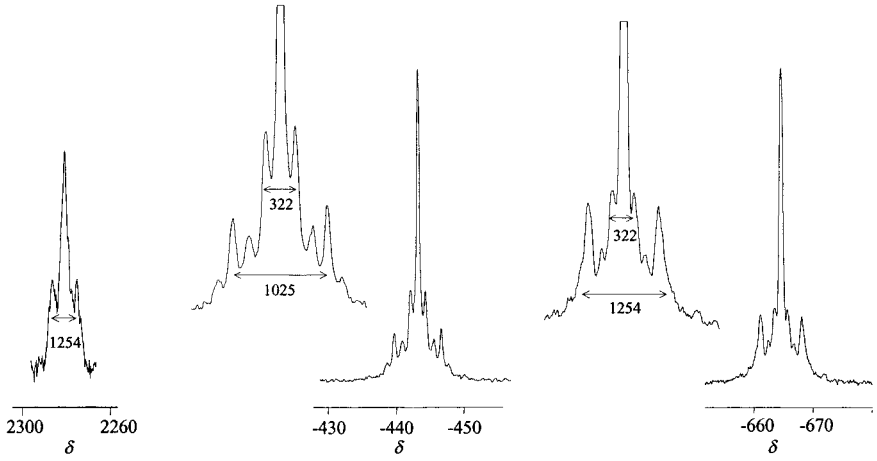

Figure 4. ^{119}Sn NMR spectra for the $[Sn_9W(CO)_3]^{4-}$ ion (**3**). Data were recorded at 298 K at 186.5 MHz in DMF.

terns indicates that the ^{183}W–^{119}Sn couplings are not responsible for any of the major features in the spectral lines in **3**. The resonance for the bottom capping position, Sn(9), is shifted by 291 ppm to higher field for the Mo complex relative to **3**.

The exchange between the η^4 and η^5 isomers can be viewed as a triangular face rotation about the four top faces of the *closo* structure that effectively moves the $\{M(CO)_3\}$ fragment between the top capping position and the four positions of the top waist site (see Scheme 2). The actual mechanism of exchange most likely results from successive diamond–square–diamond transformations involving single bond-breaking/bond-making steps.[38] The NMR spectrum reflects the highest symmetry conformation in the process, which are the C_{4v} structures observed for **1**–**3**. Four important points to note are: 1) the $\{M(CO)_3\}$ fragment only migrates between the *top* capping position and *top* waist positions; 2) the four Sn atoms within the bottom waist become equivalent by the $\{M(CO)_3\}$ scrambling process, but do not move themselves; 3) Sn(9) is not involved in the exchange process and the bonds to Sn(9) are never broken; and 4) the scrambling remains rapid at $-50\,^{\circ}$C in DMF.

The ^{119}Sn NMR spectral properties of **1**–**3** are affected in several ways by the exchange process. The most evident ramification is the simplification of the spectrum itself, which appears as a three line pattern instead of the expected six resonance pattern (based on the X-ray results for **3**). In fact, without the knowledge of the η^5 isomer from the solid state X-ray diffraction study of **3**, one would most likely conclude that compounds **1**–**3** were static with the η^4 capping structure. The second consequence of the equilibrium is that the chemical shifts and coupling constants are both temperature and solvent dependent (see Table 4 in the Supporting Information). The observed spectral resonances represent the equilibrium-weighted concentrations of the η^4 and η^5 isomers, which gives rise to coupling constants that are also weighted averages of these limiting structures. Because we cannot observe the spectrum of either limiting structure (they are always in fast exchange), we can only measure effective chemical shifts and coupling constants under a given set of conditions. Therefore, the NMR data for **1**–**3** recorded in DMF and en/tol mixtures given in Table 4 in the Supporting Information do not represent either of the limiting species. Moreover, the chemical shifts and, more importantly, the tin–tin coupling constants observed from liquid NH_3 solutions[29] are significantly different from the data given in the table. These studies will be described by Schrobilgen et al. in a subsequent publication.[29] Finally, despite the fact that 1) the three crystallographic forms of **1** that have been characterized in the solid state have the η^4 structure, 2) the solid-state IR data for **1** shows only the η^4 structure, and 3) NMR data are consistent with the η^4 structure, it is possible that the $\eta^4 \rightleftarrows \eta^5$ equilibrium also exists for this cluster as well. This finding is based on the observation that the chemical shifts and coupling constants for **1** show the same solvent and temperature dependencies observed for **2** and

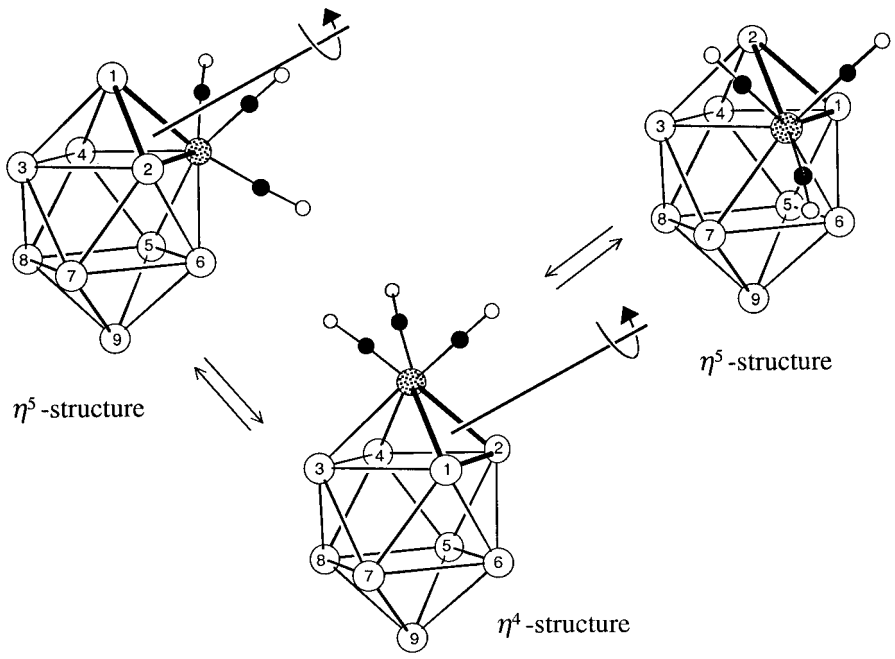

Scheme 2.

  0947-6539/01/0724-5282 $ 17.50+.50/0 *Chem. Eur. J.* **2001**, *7*, No. 24

3. The resonances for **1** differ in appearance from those of **2** and **3**, which may reflect the different equilibrium positions for the different clusters. Because the radius of Cr is smaller than that of Mo and W, complex **1** presumably prefers an η^4 coordination more than the others. Importantly, the $^1J(^{119}Sn,^{119/117}Sn)$ values between the top and bottom waist atoms are small relative to the $^1J(^{119}Sn,^{119/117}Sn)$ couplings to the capping tin atom, Sn(9). We propose that the diminished coupling constants are due, in part, to the averaging of one-bond and two-bond couplings owing to the equilibrium between the η^4 and η^5 isomers. Since Sn(9) does not get involved in the exchange process, its coupling constants are more akin to those in the static Sn_6^{2-} ion.[25]

The solid-state infrared data for compounds **1**–**3** are given in the Experimental Section and in Table 4 in the Supporting Information. The carbonyl regions of the spectra are characterized by the familiar $a_1 + e$ bands associated with the virtual C_{3v} symmetry of the $\{M(CO)_3\}$ fragments. The frequencies of the CO stretching vibrations are red-shifted relative to the neutral $[(\eta\text{-}C_6H_6)Cr(CO)_3]$ precursor and the related $[E_7M(CO)_3]^{3-}$ ions, in which E = P, As, Sb; M = Cr, Mo, W.[31] Downfield carbonyl ^{13}C NMR chemical shifts are also observed and are similar to those of the $[E_7M(CO)_3]^{3-}$ ions. Of note, the carbonyl chemical shifts of Mo and W homologues are virtually identical, which is in contrast to the usual $\Delta\delta$ shift of 7–12 ppm for similar homologues.[31, 34, 35] Again, the position of the equilibrium for the two complexes could be responsible for the anomalous trends.

As mentioned previously, the η^4 and η^5 isomers of **3** co-crystallize from solution, and we have not been able to isolate the η^5 complex in pure form. However, by indexing multiple single crystals by single-crystal X-ray diffraction from different crystalline mixtures and comparing the corresponding IR spectra, we can unequivocally assign the carbonyl bands for the η^5 complex ($\nu_{CO} = 1805$, 1701 cm^{-1}) and the η^4 complex ($\nu_{CO} = 1822$, 1705 cm^{-1}). For example, THF/en solvent mixtures yield crystals of the η^4 complex almost exclusively,[29] whereas tol/en solvent mixtures produce crystalline mixtures rich in the η^5 complex (see Figure 5). It is interesting to note

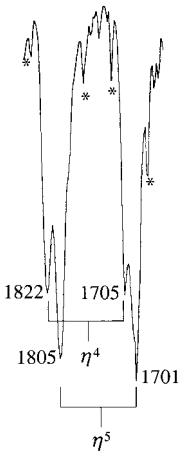

Figure 5. IR spectrum (KBr pellet) of crystalline $[K(2,2,2\text{-crypt})]_4[Sn_9W(CO)_3]$ showing the approximate 1:2 ratio of η^4 and η^5 isomers. The wave numbers for the peaks are given in cm^{-1}. The asterisks denote bands from the solvate. This sample was used in the ^{13}C NMR experiment.

that the carbonyl bands for the η^5 complex are red-shifted relative to those of the η^4 complex; this suggests a higher localization of negative charge on the W atom of the former.

Discussion

The formation of the η^5 structure for *closo*-$[Sn_9M(CO)_3]^{4-}$ ions is not so surprising in view of the various isomeric forms of metallacarboranes[36–38] that have been isolated; however, the dynamic behavior of these complexes is unexpected. Previous studies on the $[(\eta\text{-}C_7H_8)Nb(cyclo\text{-}Sn_6)Nb(\eta\text{-}C_7H_8)]^{2-}$[26] and *closo*-$[Sn_6\{Cr(CO)_5\}_6]^{2-}$[25] ions showed static behavior as expected based on the rigid structure types. In contrast, the *nido*-Sn_9^{4-} ion is highly fluxional due to a low-energy exchange process requiring little atomic reorganization (see Scheme 1). The actual mechanism of the dynamic exchange process for **1**–**3** presumably involves a reversible insertion of the $\{M(CO)_3\}$ fragment into the Sn–Sn bonds of the η^4 structure along the top waist of the cluster to generate the η^5 structure. The subsequent de-insertion must involve moving a capping Sn atom to a waist position in order to maintain the requisite two four-coordinate vertices in the *closo* structure. This process is equivalent to the diamond–square–diamond process that is operative in many metallocarboranes.[38] Moving the "bottom cap" (e.g., Sn(9), Scheme 2) into a waist position would require significant atomic reorganization and is apparently a higher energy process. As a result, the η^4–η^5–η^4 insertion/de-insertion process scrambles *only* the four top Sn atoms in the η^5 structure to give the observed time-averaged behavior. The *effective* rotation about the deltahedral faces (Scheme 2) appears to be unique to transition metal Zintl ion clusters in that it requires a vertex with reversible coordination geometries and relatively weak intervertex bonding. Dynamic vertex exchange in the metallated ten-vertex carborane $[2\text{-}(\eta^6\text{-}C_6Me_6)\text{-}closo\text{-}2,1,6\text{-}RuC_2B_7H_9]$ also occurs with a low activation barrier.[38] In the carborane, a twisting diamond–square–diamond exchange pathway is proposed in which the transition-state structure is similar to the η^5 solid-state structure of **3**. Interestingly, the authors can rule out a triangular-face rotation process due to the pair-wise vertex exchange observed by NMR spectroscopy.[38] The fluxional process for the present complexes is clearly quite different. Although complexes **1**–**3** are not static, the insertion of the $\{M(CO)_3\}$ groups to the *nido*-Sn_9^{4-} ion blocks the global exchange of the vertices leaving only localized fluxionality.

The equilibrium involving the η^4 and η^5 structures for **1**–**3** are solvent and, presumably, metal dependent; however, we are unable to measure the values of the equilibrium constants by ^{119}Sn NMR spectroscopy. The relative concentrations of the η^4 and η^5 isomers in solution could, in theory, be determined from solution IR studies. However, the only viable solvents (en, DMF, CH_3CN) have bands in the carbonyl regions of these complexes which hinders analysis. Moreover, the CO bands are significantly shifted by solvation and assignments in solution are not straightforward. Anecdotal evidence suggests that the equilibrium for the Cr complex **1** favors the η^4 structure, whereas the Mo and W complexes **2**

and **3** appear to be more thermoneutral. This proposal is based on the different appearance of the ^{119}Sn NMR spectrum of **1** relative to **2** and **3** and because the size of Cr is smaller than that of W or Mo, which should favor the lower coordination of the η^4 structure. For **2** and **3**, the relative *in*sensitivity of the Sn–Sn coupling constants to temperature in DMF suggests that the equilibrium in DMF is relatively thermoneutral. There is a much more pronounced dependence on solvent (see Table 4 in the Supporting Information and ref. [29]).

Finally, it is interesting to note that, although the complexes retain some degree of fluxionality that requires rapid and reversible Sn–Sn bond-breaking and bond-making steps, the values of the Sn–Sn coupling constants are significantly larger than those of the *nido*-Sn_9^{4-} ion ($^1J(^{119}Sn,^{117}Sn) = 254$ Hz) and other globally fluxional systems.[12, 15, 27] However, the one-bond couplings for **1**–**3** are less than those of the static *closo*-Sn_6^{2-} ions of the $[\{M(CO)_5\}_6Sn_6]^{2-}$ complexes ($^1J(^{119}Sn,^{117}Sn) = 1740-1848$ Hz)[25] and the $[(\eta\text{-}C_7H_8)Nb(\textit{cyclo}\text{-}Sn_6)Nb(\eta\text{-}C_7H_8)]^{2-}$ ion ($^1J(^{119}Sn,^{117}Sn) = 1975$ Hz).[26] Further studies on these and other metallated polystannides are in progress.

Experimental Section

General data: All reactions were performed in a nitrogen atmospheres dry box (Vacuum Atmospheres Company). ^{119}Sn NMR spectra were recorded on Bruker DRX500 AVANCE and AM400 AVANCE spectrometers operating at 186.5 MHz and 149.2 MHz, respectively. ^{119}Sn chemical shift was referenced to Me_4Sn in C_6D_6 (0 ppm). IR spectra were recorded from KBr pellets on a Nicolet 560 FTIR spectrometer. Elemental analyses were performed under inert atmospheres by Atlantic Microlab, Norcross, GA.

Chemicals: Melts of nominal composition K_4Sn_9 were made by high-temperature fusion (1000 °C) of stoichiometric ratios of the elements. The chemicals were sealed in evacuated, silica tubes and carefully heated with a natural gas/oxygen flame. 4,7,13,16,21,24-Hexaoxa-1,10-diazobicyclo[8.8.8]-hexacosane (2,2,2-crypt), (cycloheptatriene)molybdenum tricarbonyl, (mesitylene)chromium tricarbonyl, and (mesitylene)tungsten tricarbonyl were purchased from Aldrich. Anhydrous ethylenediamine (en) and dimethylformamide (DMF) were purchased from Fisher, vacuum distilled from K_4Sn_9 and stored under dinitrogen. Toluene was distilled from sodium/benzophenone under dinitrogen and stored under dinitrogen.

Preparation of [K(2,2,2-crypt)]$_4$[Sn$_9$Cr(CO)$_3$]·en: This synthesis is a modification of the previously published procedure.[23] In vial 1, K_4Sn_9 (100 mg, 0.082 mmol) was dissolved in en (ca. 2 mL) to produce a red solution. In vial 2, $[Cr(CO)_3\{C_6H_3(CH_3)_3\}]$ (21 mg, 0.082 mmol) was dissolved in toluene (ca. 1 mL) to produce a yellow solution. The contents of vial 2 were added to the contents of vial 1, and four equivalents of crypt (120 mg, 0.32 mmol) were added as a solid. The reaction mixture was stirred for 2 h to yield a dark green-brown solution. The reaction mixture was then filtered through tightly packed glass wool in a pipet. Dark red crystals formed in the reaction vessel after 4 days (56 mg, 24 %). ^{119}Sn NMR (149.2 MHz, DMF, 25 °C): $\delta = -180$ ($J(^{119}Sn,^{119/117}Sn) = 354$, 556, 878 Hz), -447 ($J(^{119}Sn,^{119/117}Sn) = 354$, 878, 1240 Hz), 2327 ($J(^{119}Sn,^{119/117}Sn) = 354$, 1240 Hz); ^{13}C NMR (100 MHz, DMF, 25 °C): $\delta = 244$; IR (KBr): $\tilde{\nu} = 1822$, 1705 cm^{-1} (CO).

Preparation of [K(2,2,2-crypt)]$_4$[Sn$_9$Mo(CO)$_3$]·1.5en: In vial 1, K_4Sn_9 (90 mg, 0.074 mmol) was dissolved in en (ca. 2 mL) to produce a red solution. In vial 2, $[Mo(CO)_3(C_7H_8)]$ (20 mg, 0.074 mmol) was dissolved in toluene (ca. 1 mL) and gently heated to give a red solution. Some of the molybdenum complex did not dissolve in the toluene. The contents of vial 2, including the undissolved Mo complex were added to the contents of vial 1, to give a red solution. Four equivalents of crypt (111 mg, 0.29 mmol) was added as a solid, and the reaction mixture was stirred for 2 h to yield a dark green-brown solution. The reaction mixture was filtered through tightly packed glass wool in a pipet. Dark red crystals formed in the reaction vessel after 24 h (48 mg, 22 %). ^{119}Sn NMR (149.2 MHz, DMF, 25 °C): $\delta = -361$ ($J(^{119}Sn,^{119/117}Sn) = 358$, 677, 1065 Hz), -606 ($J(^{119}Sn,^{119/117}Sn) = 358$, 677, 1065, 1252 Hz), 1988 ($J(^{119}Sn,^{119/117}Sn) = 358$, 1252 Hz); ^{13}C NMR (100 MHz, DMF, 25 °C): $\delta = 240$; IR (KBr): $\tilde{\nu} = 1829$, 1708 cm^{-1} (CO); elemental analysis calcd (%) for $K_4Sn_9MoC_{78}H_{156}O_{27}N_{11}$: C 31.2, H 5.2, N 5.1; found: C 29.54, H 5.04, N 4.88.

Preparation of [K(2,2,2-crypt)]$_4$[Sn$_9$W(CO)$_3$]·1.5en: In vial 1, K_4Sn_9 (80 mg, 0.065 mmol) was dissolved in en (ca. 2 mL) to produce a red solution. In vial 2, $[W(CO)_3\{C_6H_3(CH_3)_3\}]$ (25 mg, 0.065 mmol) was dissolved in toluene (ca. 1 mL) and gently heated to give a green solution. The contents of vial 2 were added to the contents of vial 1, to produce a brown-green solution. Four equivalents of crypt (98 mg, 0.26 mmol) were added as a solid, and the reaction mixture was stirred for 6 h to yield a dark brown solution with a dark precipitate. The reaction mixture was heated gently (ca. 60 °C) to dissolve the precipitate. While hot, the resulting dark red solution was filtered through tightly packed glass wool in a pipet. Dark red crystals formed in the reaction vessel after 24 h (43 mg, 22 %). ^{119}Sn NMR (149.2 MHz, DMF, 25 °C): $\delta = -443$ ($J(^{119}Sn,^{119/117}Sn) = 322$, 665, 1025, 1326 Hz), -662 ($J(^{119}Sn,^{119/117}Sn) = 322$, 665, 1025, 1254 Hz), 2279 ($J(^{119}Sn,^{119/117}Sn) = 322$, 1254 Hz); ^{13}C NMR (100 MHz, DMF, 25 °C): $\delta = 239$; IR (KBr): $\tilde{\nu} = 1805$, 1701 cm^{-1} (CO); elemental analysis calcd (%) for $K_4Sn_9WC_{77}H_{152}O_{27}N_{10}$: C 30.25, H 4.97, N 4.58; found: C 30.43, H 5.02, N 4.35.

Rate analysis for η^4–η^5 conversion: A procedure identical to that described for the synthesis of $[K(2,2,2\text{-crypt})]_4[Sn_9W(CO)_3]$ was used. The resulting solution was evaporated to dryness after 14 days. The resulting dark red solid was analyzed as KBr pellets showing > 90 % [η^4-$Sn_9W(CO)_3]^{4-}$.

Crystallographic studies

[K(2,2,2-crypt)]$_4$[1]·1.5en: A dark block with dimensions $0.296 \times 0.243 \times 0.175$ mm^3 was placed and optically centered on the Bruker SMART CCD system at -80 °C. The initial unit cell was indexed by using a least-squares analysis of a random set of reflections collected from three series of 0.3° wide ω scans (25 frames per series) that were well distributed in reciprocal space. Data frames were collected [$Mo_{K\alpha}$] with 0.3° wide ω scans, 20 seconds per frame, 606 frames per series. Five complete series were collected with an additional 200 frames, a repeat of the first series for redundancy and decay purposes, with a crystal to detector distance of 4.935 cm, thus providing a complete sphere of data to $2\theta_{max} = 55.0°$. A total of 90485 reflections were collected (26037 unique; $R(\text{int}) = 0.0347$) and corrected for Lorentz and polarization effects and absorption by using Blessing's method as incorporated into the program SADABS.

The SHELXTL program package was implemented for data processing, structure solution, and refinement. System symmetry, lack of systematic absences, and intensity statistics indicated the centrosymmetric triclinic space group $P\bar{1}$ (no. 2). The structure was determined by direct methods with the successful location of the heavy atoms comprising the cluster. After several difference Fourier refinement cycles, all of the atoms were located, refined isotropically and then anisotropically. Hydrogen atoms on the cryptand molecules were placed in calculated positions and later had their thermal parameters refined. Ethylenediamine hydrogen atoms were calculated and their thermal parameters were dependent upon parent. An empirical correction for extinction was also attempted but found to be negative and therefore not applied. The final structure was refined to convergence [$\Delta/\sigma \leq 0.001$]. A final difference Fourier map was featureless indicating the structure is therefore both correct and complete.

[K(2,2,2-crypt)]$_4$[3]·1.5en: A dark red block with dimensions $0.183 \times 0.091 \times 0.055$ mm^3 was mounted in a drybox and was placed and optically centered on the Bruker SMART CCD system at -80 °C. Data were processed and the structure determined and refined as described above. After several difference Fourier refinement cycles, all of the atoms were located, refined isotropically, then anisotropically. Two ethylenediamine molecules were located with the first being disordered (occupancies 0.6:0.4) and the second position partially occupied about a special position. A disorder involving a second orientation of the $[Sn_9W(CO)_3]^{3-}$ cluster at the same site was found and successfully modeled in which the major:minor orientations had occupancies 0.83:0.17, respectively. Hydrogen atoms were placed in calculated positions with their thermal parameters dependent

  0947-6539/01/0724-5284 $ 17.50+.50/0 *Chem. Eur. J.* **2001**, *7*, No. 24

upon the parent atom. The final structure was refined to convergence [$\Delta/\sigma \leq 0.001$] with $R(F) = 13.09\,\%$, $wR(F^2) = 16.93\,\%$, GOF = 1.077 for all 2049 unique reflections [$R(F) = 5.92\,\%$, $wR(F^2) = 12.71\,\%$ for those 11303 data with $F_o > 4\sigma(F_o)$]. A final difference Fourier map was featureless indicating the structure is therefore both correct and complete.

Crystallographic data (excluding structure factors) for the structures reported in this paper have been deposited with the Cambridge Crystallographic Data Centre as supplementary publication no. CCDC-168788, CCDC-168789, and CCDC-168790. Copies of the data can be obtained free of charge on application to CCDC, 12 Union Road, Cambridge CB2 1EZ, UK (fax: (+44) 1223-336-033; e-mail: deposit@ccdc.cam.ac.uk).

Acknowledgement

This work was supported by the Petroleum Research Fund of the American Chemical Society. We thank Dr. Yiu Fai Lam for assistance with the ^{119}Sn NMR studies.

[1] A. Joannis, *C. R. Hebd. Seances Acad. Sci.* **1891**, *113*, 795.
[2] A. Joannis, *C. R. Hebd. Seances Acad. Sci.* **1892**, *114*, 585.
[3] C. A. Kraus, *J. Am. Chem. Soc.* **1907**, *29*, 1557.
[4] C. A. Kraus, *J. Am. Chem. Soc.* **1922**, *44*, 1216.
[5] F. H. Smyth, *J. Am. Chem. Soc.* **1917**, *39*, 1299.
[6] E. Zintl, A. Harder, *Z. Phys. Chem. Abt. A* **1931**, *154*, 47.
[7] E. Zintl, J. Goubeau, W. Dullenkopf, *Z. Phys. Chem. Abt. A* **1931**, *154*, 1.
[8] E. Zintl, W. Dullenkopf, *Z. Phys. Chem. Abt. B* **1932**, *16*, 183.
[9] E. Zintl, H. Kaiser, *Z. Anorg. Allg. Chem.* **1933**, *211*, 113.
[10] L. Diehl, K. Khodadedeh, D. Kummer, J. Strähle, *Chem. Ber.* **1976**, *109*, 3404.
[11] J. D. Corbett, P. A. Edwards, *J. Am. Chem. Soc.* **1977**, *99*, 3313.
[12] J. D. Corbett, *Chem. Rev.* **1985**, *85*, 383.
[13] K. J. Wade, *Adv. Inorg. Chem. Radiochem.* **1976**, *18*, 1.
[14] R. W. Rudolph, W. L. Wilson, F. Parker, R. C. Taylor, D. C. Young, *J. Am. Chem. Soc.* **1978**, *100*, 4629.
[15] W. L. Wilson, R. W. Rudolph, L. L. Lohr, R. C. Taylor, P. Pyykko, *Inorg. Chem.* **1986**, *25*, 1535.
[16] T. F. Fassler, *Coord. Chem. Rev.* **2001**, *215*, 347.
[17] S. C. Critchlow, J. D. Corbett, *J. Am. Chem. Soc.* **1983**, *105*, 5715.
[18] T. F. Fassler, R. Hoffmann, *Z. Kristallogr. New Cryst. Struct.* **2000**, *215*, 139.
[19] P. A. Edwards, J. D. Corbett, *Inorg. Chem.* **1977**, 903.
[20] R. W. Rudolph, W. L. Wilson, R. C. Taylor, *J. Am. Chem. Soc.* **1981**, *103*, 2480.
[21] T. F. Fassler, S. Hoffmann, *Z. Kristallogr.* **1999**, *214*, 722.
[22] H. G. von Schnering, M. Baitinger, U. Bolle, W. CarrilloCabrera, J. Curda, Y. Grin, F. Heinemann, J. Llanos, K. Peters, A. Schmeding, M. Somer, *Z. Anorg. Allg. Chem.* **1997**, *623*, 1037.
[23] B. W. Eichhorn, R. C. Haushalter, W. T. Pennington, *J. Am. Chem. Soc.* **1988**, *110*, 8704.
[24] B. Schiemenz, G. Huttner, *Angew. Chem.* **1993**, *105*, 295; *Angew. Chem. Int. Ed. Engl.* **1993**, *32*, 297.
[25] G. Renner, P. Kircher, G. Huttner, P. Rutsch, K. Heinze, *Eur. J. Inorg. Chem.* **2001**, 973.
[26] B. Kesanli, B. W. Eichhorn, J. C. Fettinger, *Angew. Chem.* **2001**, *113*, 2364; *Angew. Chem. Int. Ed.* **2001**, *40*, 2300.
[27] F. Teixidor, M. L. Leutkens, Jr., R. W. Rudolph, *J. Am. Chem. Soc.* **1983**, *105*, 149.
[28] B. Kesanli, B. W. Eichhorn, J. C. Fettinger, unpublished results.
[29] G. Schrobilgen, H. Mercier-Schrobilgen, personal communication, **2001**.
[30] The "Wadian" name for this cluster would be [1,1,1-(CO)$_3$-*closo*-1-CrSn$_9$]$^{4-}$.
[31] S. Charles, S. G. Bott, A. L. Rheingold, B. W. Eichhorn, *J. Am. Chem. Soc.* **1994**, *116*, 8077.
[32] Crystal data for [K(2,2,2-crypt)]$_4$[Sn$_9$Mo(CO)$_3$]·1.5en: $a = 15.6802(22)$, $b = 16.0730(22)$, $c = 26.0397(35)$ Å; $\alpha = 94.552(3)^\circ$, $\beta = 90.462(3)^\circ$, $\gamma = 118.341(3)^\circ$; $V = 5750.0(23)$ Å^3.
[33] The "Wadian" name for this cluster would be [2,2,2-(CO)$_3$-*closo*-2-WSn$_9$]$^{4-}$
[34] P. S. Braterman, D. W. Milne, E. W. Randall, E. Rosenberg, *J. Chem. Soc. Dalton Trans.* **1973**, 1027.
[35] M. Y. Darensbourg, S. Slater, *J. Am. Chem. Soc.* **1981**, *103*, 5914.
[36] J. Bould, J. D. Kennedy, M. Thorntonpett, *J. Chem. Soc. Dalton Trans.* **1992**, 563.
[37] M. Brown, X. L. R. Fontaine, N. N. Greenwood, J. D. Kennedy, P. Mackinnon, *J. Chem. Soc. Chem. Commun.* **1987**, 817.
[38] M. Bown, T. Jelinek, B. Stibr, S. Hermanek, X. L. R. Fontaine, N. N. Greenwood, J. D. Kennedy, M. Thorntonpett, *J. Chem. Soc. Chem. Commun.* **1988**, 974.

Received: June 26, 2001 [F3372]